X-695-77-32

PREPRINT

TMX 71384

AN EXTENSION OF DUAL MAGNETOMETER METHOD FOR USE ON A DUAL SPINNING SPACECRAFT

R. P. LEPPING
N. F. NESS

FEBRUARY 1977

GSFC — GODDARD SPACE FLIGHT CENTER —
GREENBELT, MARYLAND

X-695-77-32

AN EXTENSION OF THE DUAL MAGNETOMETER METHOD FOR USE ON A DUAL SPINNING SPACECRAFT

BY

R. P. Lepping
N. F. Ness

Laboratory for Extraterrestrial Physics
NASA/Goddard Space Flight Center
Greenbelt, Maryland 20771

January 1977

Short Title: Extension of Dual Magnetometer Method

ABSTRACT

A method of estimating and correcting for the magnetic field of a dual spinning spacecraft has been developed by employing an extension of the dual magnetometer technique of Ness et al. (1971). This new method is useful for those situations in which a magnetometer boom of modest length (7-10m) is attached to the spinning part of a large spacecraft (800-1000 Kg). The purpose of using a dual spinning spacecraft is to accommodate two types of instruments: (1) imaging and similar "pointed" remote sensing systems on the stationary platform and (2) fields, particles and other in-situ measuring instruments on the spinning portion. Present-day imaging systems are well known to exhibit large magnetic moments, sometimes displaced from the spacecraft center by a significant amount. The new method assumes that the stationary part of the spacecraft possesses a magnetic field which is represented by a combination of a dipole and a quadrupole field.

INTRODUCTION

It is well known that the existence of a spacecraft magnetic field can be a predominant source of magnetometer measurement error if not properly taken into account (Ness, 1970). This is especially of concern for the class of larger spacecraft constructed with minimal magnetic constraints, which invariably produce significant fields. In this paper we discuss this serious and continuing problem and develop a method of reducing the effects of this contamination field. This new method is an extension of a scheme developed earlier which uses simultaneous dual magnetometer measurements (Ness et al., 1971). It is applicable to dual spinning spacecraft which possess both a "stationary" segment and a spinning segment.

If the net instantaneous spacecraft field in-flight can be approximated near the end of the magnetometer boom as that of a spacecraft-centered, tilted dipole, the dual magnetometer method of correcting the measured field can be easily employed in the same manner as was first successfully used on the Mariner 10 spacecraft (described in general by Ness et al., 1971, and specifically by Lepping et al., 1975). Briefly, at the end of a 6 meter boom, the Mariner 10 spacecraft field varied from 1-4γ depending upon the orientation of the imaging system (Ness et al., 1974).

The magnetic field of an on-board imaging system is known to be appreciable, because it contains invar rods used for lens alignment, and invar is a magnetically soft metal capable of being easily magnetized by the focusing field or other external fields. The

imaging system is often offset from the spacecraft center and this can be a significant fraction of the boom length. Under these conditions, it is obvious that the possibility of a relatively strong quadrupole moment will exist, as seen at the positions of the dual magnetometer sensors.

The method proposed here employs a centered dipole-plus-quadrupole field model for the stationary part of the spacecraft field and a centered rotating dipole model for the spinning portion. The principal contribution to the quadrupole moment is expected to come from the field of the imaging system, but other much weaker contributers also will exist. This complex field of the stationary part of the spacecraft is seen by each triaxial magnetometer as rotating through 360° every spin of the spacecraft, since the magnetometer boom is attached to the spinning part. Therefore, during one spin period both magnetometers obtain many measurements of this stationary field plus the ambient field and the field of the spinning spacecraft (which appears stationary at the sensor positions). It is possible to accurately estimate the ambient field for each measurement if one can subtract from the measured field an accurate estimate of the total spacecraft field.

For fluxgate magnetometers, intrinsic zero offsets can be determined in flight continuously by use of mechanical and electronic flippers. The incremental magnetic field obtained by taking the instantaneous difference between the inner and outer magnetometer measurements is then a function of only the net

spacecraft field for each angle ϕ at which a measurement is made (ϕ being the azimuthal angle measured in the equatorial plane of the spacecraft). Below we develop a detailed formulation of an extension of the dual magnetometer method, called here for short the "dipole-quadrupole method", and discuss the results of some tests of its performance by applying it to many different spacecraft magnetic field configurations.

FORMULATION OF THE METHOD

A second order spherical harmonic expansion is assumed to approximate well the stationary spacecraft field at the position of the dual magnetometers. [This "fixed" field is seen as spinning by the magnetometer sensors.] It is assumed that the magnetometer boom is perpendicular to the spin axis of the spacecraft and that the intersection of the boom line with the spin axis is very close to the spacecraft's center of gravity. Therefore, this intersection point is a natural choice for the center of our coordinate system and likewise, the spin axis is chosen to be the polar axis. Hence, measurements are made at $\theta = 90^\circ$ at all times, and thus, in terms of Schmidt (1934) normalized coefficients, such an expansion will simplify to the form:

$$B_r^{(f)} = 2\left(\frac{a}{r}\right)\left[g_1^1\cos\phi + h_1^1\sin\phi\right] + 3/2\left(\frac{a}{r}\right)^4\left[-g_2^0 + \sqrt{3}\left(g_2^2\cos 2\phi + h_2^2\sin 2\phi\right)\right] \quad (1)$$

$$B_\theta^{(f)} = \left(\frac{a}{r}\right)^3 g_1^0 + \left(\frac{a}{r}\right)^4 \sqrt{3}\left[g_2^1\cos\phi + h_2^1\sin\phi\right] \quad (2)$$

and

$$B_{\phi}^{(f)} = \left(\frac{a}{r}\right)^3 \left[g_1^1 \sin\phi - h_1^1 \cos\phi\right] + \left(\frac{a}{r}\right)^4 \sqrt{3}\left[g_2^2 \sin 2\phi - h_2^2 \cos 2\phi\right], \tag{3}$$

where θ and ϕ are the polar and azimuthal angles, respectively, r is the distance from the spacecraft center to the measurement position, and a is effectively the radius of the smallest sphere containing the spacecraft proper, i.e. excluding appendates.

The spinning part of the net spacecraft field appears as a fixed field in the sensor frame of reference and is assumed to be approximated by a centered, tilted dipole as:

$$B_r^{(s)} = 2\left(\frac{a}{r}\right)^3 \ell_1, \tag{4}$$

$$B_{\theta}^{(s)} = \left(\frac{a}{r}\right)^3 \ell_2, \tag{5}$$

$$B_{\phi}^{(s)} = \left(\frac{a}{r}\right)^3 \ell_3, \tag{6}$$

where $\ell_i (i = 1,2,3)$ are orthogonal components of the dipole moment. We now combine the spinning and fixed fields to obtain the total spacecraft field

$$\vec{B}^t = \vec{B}^{(f)} + \vec{B}^{(s)}, \tag{7}$$

which in cartesian coordinate representation is

$$B_x^t = 2\left(\frac{a}{r}\right)^3 \left(\ell_1 + g_1^1 \cos\phi + h_1^1 \sin\phi\right) + \frac{3\sqrt{3}}{2}\left(\frac{a}{r}\right)^4 \left(g_2^2 \cos 2\phi + h_2^2 \sin 2\phi - g_2^0/\sqrt{3}\right), \tag{8}$$

$$B_y^t = \left(\frac{a}{r}\right)^3 \left(\ell_3 + g_1^1 \sin\phi - h_1^1 \cos\phi\right) + \left(\frac{a}{r}\right)^4 \sqrt{3}\left(g_2^2 \sin 2\phi - h_2^2 \cos 2\phi\right), \tag{9}$$

and

$$B_z^t = \left(\frac{a}{r}\right)^3 \ell_4 + \left(\frac{a}{r}\right)^4 \sqrt{3}\,(g_2^1 \cos\phi + h_2^1 \sin\phi), \qquad (10)$$

where $\ell_4 = g_1^0 + \ell_2$, and the following identifications were made: $B_r^t \equiv B_x^t$, $B_\theta^t \equiv B_z^t$, and $B_\phi^t \equiv B_y^t$.

Since both the ℓ_1 and g_2^0 terms in equation 8 are independent of ϕ and depend upon r according to different power laws, the ℓ_1 and g_2^0 coefficients cannot be solved for separately using in-flight data. This would present no problem if the spinning dipole moment were negligible, because then $\ell_1 \approx 0$, and g_2^0 could be isolated and obtained numerically. In general, this will not be the case, but fortunately for many cases in practice, the g_2^0 term is found to be negligible, as shown in the Appendix. Accordingly then, the g_2^0 coefficient will be treated as negligible in the following formulation.

Consider the fields measured at the inner (1) and outer (2) magnetometer sensors, which are expressed as:

$$\vec{B}_M(1) = \vec{B}_{z0}(1) + \vec{B}^t(1) + \vec{B}_A \qquad (11)$$

and

$$\vec{B}_M(2) = \vec{B}_{z0}(2) + \vec{B}^t(2) + \vec{B}_A, \qquad (12)$$

where $\vec{B}_{z0}$ is the magnetometer's intrinsic zero offset, $\vec{B}^t$ is the net spacecraft field, and $\vec{B}_A$ is the ambient field. For accurately known zero offsets of the sensors, i.e., $\vec{B}_{z0}(j) = 0$, the difference between the inner and outer measured fields is then

$$\Delta\vec{B} = \vec{B}_M(1) - \vec{B}_M(2) = \vec{B}^t(1) - \vec{B}^t(2), \qquad (13)$$

since the ambient field cancels exactly. Using our "dipole-quadrupole model" field we finally obtain:

$$\Delta\vec{B}_x = 2R_3 (\ell_1 + g_1^1 \cos\phi + h_1^1 \sin\phi) \qquad (14)$$

$$+ \frac{3\sqrt{3}}{2} R_4 (g_2^2 \cos 2\phi + h_2^2 \sin 2\phi),$$

$$\Delta B_y = R_3(\ell_3 + g_1^1 \sin\phi - h_1^1 \cos\phi) \qquad (15)$$

$$+ R_4\sqrt{3} (g_2^2 \sin 2\phi - h_2^2 \cos 2\phi),$$

and

$$\Delta B_z = R_3\ell_4 + R_4\sqrt{3} \ (g_2^i \cos\phi + h_2^1 \sin\phi), \qquad (16)$$

where ΔB_i (i = x,y,z) are the components of the measured difference field, and

$$R_3 = (\frac{a}{r_1})^3 - (\frac{a}{r_2})^3 \qquad (17)$$

and

$$R_4 = (\frac{a}{r_1})^4 - (\frac{a}{r_2})^4 \qquad (18)$$

are exactly determined by the known positions of the inner and outer sensors.

The nine unknown coefficients in the difference equations (14, 15, 16) can be obtained in several ways. A computationally simple method, shown through simulations to be clearly adequate, is to evaluate the three difference equations at four symmetrically chosen values of $\phi(0^\circ,90^\circ,180^\circ,270^\circ$, for example) which are solved simultaneously to produce (3 x 4 =) 12 values of the 9 coefficients. Hence, three are determined redundantly. [One is free to choose other sets of four or more angles for determining the coefficients, but this

choice provides simpler analytical forms.]

Once the coefficients' values are determined for a given spacecraft spin period they are used in equations 8,9,10 for the outer sensor's position, r_2, to estimate the spacecraft field at that position, $\vec{B}^{st}(2)$. Then, equation 12 is used to estimate the ambient field, B_A, from measurements from the outer magnetometer, $\vec{B}_M(2)$, and the accurately known $\vec{B}_{zO}(2)$. The method, of course, depends on the "stationary" spacecraft field remaining quasi-static on the time scale of one spin period. Experience from the Mariner 10 mission shows that this will normally be the case for typical spin periods (6-12 sec).

EXAMPLES OF METHOD: JUPITER-ORBITER-PROBE 1981/1982

To demonstrate the utility of the method, various cases of realistically simulated JOP 81/82 spacecraft magnetic fields have been examined. In the examples we compare:

(1) the true field with

(2) the field estimated by the "dipole-quadrupole model" as outlined above, and with

(3) the centered dipole field approximation as employed in the Mariner 10 mission.

The latter field (at the outer magnetometer location) is given by

$$\vec{B}^D = \frac{\alpha \Delta \vec{B}}{1-\alpha}, \qquad (19)$$

as described by Ness et al., 1971; $\Delta\vec{B}$ is given by the first part of eq. 13 and $\alpha \equiv (r_1/r_2)^3$ is the known spatial "coupling coefficient".

In particular for the outer magnetometer location, r_2, the following quantities are calculated:

(1) the magnitude of the true spacecraft field, S_T;

(2) the magnitude of the difference between the "dipole-quadrupole model" estimated field and the true field, S_Q; and

(3) the magnitude of the difference between the dipole estimated field and the true field, S_D.

First, we calculate these quantities as functions of ϕ for two different boom lengths, 6 and 9 m. In both cases the true spacecraft field is simulated by three dipoles whose characteristics and locations are given in Table 1 where η is a latitude angle, i.e. the inclination from the equatorial plane. These characteristics are realistic, based on:

a) our general knowledge of possible field strengths of spacecraft subsystems in combination,

b) our experience with Mariner 10, and

c) the results of field mappings of the MJS'77 spacecraft which have transpired to this date.

Figure 1 shows the results of these simulation tests. For the case of the 6 m boom, the locations of the inner and outer sensors from the spinning spacecraft center are r_1 = 4.7 m and r_2 = 7.0 m, consistent for a 6 m boom and a spacecraft radius plus strut length of approximately 1 m. This case is designated with a "7" in the figure. In the case of the 9 m boom, similarly, r_1 = 7.0 m and r_2 = 10.0 m; this is designated with a "10" in the figure.

TABLE 1

Simulated Field Characteristics

Imaging System Dipole. (Angle estimates based on J.P.L. 660-22, JOP 81/82 Orbiter Description Document.)	$\lvert\vec{M}_{IS}\rvert$ = 1000 gauss cm^3	
	τ_{IS} = 15°	in fixed system
	ϕ_{IS} = 0°	
Stationary "axial" dipole moment (center of stationary moment is distance D above spinning center, along spin axis).	$\lvert\vec{M}_S\rvert$ = 150 gauss cm^3	
	τ_S = 80°	in fixed system
	ϕ_S = 90°	
	D = 0.5 m	
Spinning centered dipole moment. (This point is at intersection of spin axis and boom line.)	$\lvert\vec{M}_C\rvert$ = 250 gauss cm^3	
	τ_C = 45°	in spinning system
	ϕ_C = 45°	
Displacement vector between the spinning center and the imaging system moment's center. (Estimates based on JOP Description Document; see above.)	R = 1.6 m	
	τ_R = 45°	
	ϕ_R = 0°	

For the 7.0 m case (thin lines) figure 1 shows an unacceptably large S_T (thin dotted) for the entire 360° range of ϕ reaching $\approx 1\ \gamma$ at $\phi = 0^\circ$. This must be considered an error field if a dual magnetometer method is not employed. S_D (thin dashed) shows a distinct improvement over S_T for all ϕ. S_Q (thin solid) is $\leq 0.15\ \gamma$ for all ϕ representing an improvement over S_D of better than a factor of ≈ 3 or an improvement over S_T of better than 6 at $\phi = 0^\circ$, the worst case position.

Similarly for the 10.0 m case (heavy lines) we see that for $\phi = 0^\circ$ the maximum S_T (heavy dotted) is $0.29\ \gamma$, S_D (heavy dashed) is $0.07\ \gamma$ and S_Q (heavy solid) is $0.02\ \gamma$ giving improvement factors of $S_T/S_D = 4.4$ and $S_T/S_Q = 14$. So, even in the case of the longer boom (standoff 10.0 m) for this spacecraft field, S_T is unacceptable (i.e. $> 0.025\ \gamma$) at all ϕ, and S_D is unacceptable for almost half the cycle. Only S_Q remains below $0.025\ \gamma$ for all ϕ. As can be seen, the $\phi = 0^\circ$ position is where S_T and S_D are maximum and therefore is the worst case position; this is true for any simulated field since the displacement vector of the imaging system is chosen to be in the $\phi = 0^\circ$ meridian plane. Therefore, the relative merits of the two methods can be determined satisfactorily by comparing their results for the $\phi = 0^\circ$ position only.

In Table 2 we show the results of ten tests where the input values of M_{IS}, M_C and M_S are varied but all the other input parameter values are the same as those used in obtaining Figure 1. Odd and even number tests correspond to short (6 m) and moderate (9 m) length

booms, respectively. The first two rows in the table, tests 1 and 2, are identical to those in the figure for all input parameters. Notice that the $r_2 = 10$ m cases produce values of $S_Q \leq 0.025\ \gamma$, indicating that a combination of a moderate length boom and the new dipole-quadrupole method will always yield acceptably small errors. Tests 1 and 3 differ only in that M_C is slightly larger in test 1 where expectedly S_T is slightly larger, but S_D is equal for the two tests and likewise for S_Q. The same comment holds for tests 2 and 4. In fact, S_D and S_Q are independent of M_C since either method exactly subtracts out the spinning centered dipole. In reality, how well this holds depends on how well the centered dipole approximates the spinning spacecraft field.

Notice that S_D for test 1 is approximately equal to S_T for test 2, and likewise for all even-odd test pairs. This demonstrates for the particular simulated net spacecraft field chosen, that applying the centered dipole field approximation of Ness et al. (1971) is equivalent to lengthening the boom by 3 m and applying no correction method. Similarly S_Q for test 1 is approximately one half S_T for test 2 and likewise for all even-odd pairs. This means that applying the new dipole-quadrupole method of approximating the field yields a decrease in error by a factor of about 2 over lengthening the boom by 3 m and applying no correction method.

The odd numbered tests, where the boom is short, yield modest improvement factors S_T/S_Q of ≈ 6, and the even number tests, where the boom is of moderate length, yield large improvement factors

TABLE 2

Spacecraft Field Error Estimates

Test No.	Dipole Moments gauss cm^3			Standoff Distance (meters)		Field Error Estimates (γ) at $\phi=0^\circ$			Improvement Factors	
	M_{IS}	M_C	M_S	r_1	r_2	S_T	S_D	S_Q	S_T/S_D	S_T/S_Q
1	1000	250	150	4.7	7	0.92	0.33	0.15	2.8	6.1
2	1000	250	150	7	10	0.29	0.07	0.02	4.4	14
3	1000	150	150	4.7	7	0.90	0.33	0.15	2.7	6.0
4	1000	150	150	7	10	0.28	0.07	0.02	4.3	14
5	800	300	200	4.7	7	0.76	0.26	0.13	2.9	5.8
6	800	300	200	7	10	0.24	0.05	0.02	5.4	15
7	500	250	150	4.7	7	0.49	0.16	0.08	3.1	6.1
8	500	250	150	7	10	0.15	0.03	0.01	4.8	15
9	500	150	150	4.7	7	0.47	0.16	0.08	2.9	5.9
10	500	150	150	7	10	0.15	0.03	0.01	4.5	15

$S_T/S_Q \approx 15$. This shows that the ratio S_T/S_Q (as well as S_T/S_D) itself increases as the boom is lengthened, just as the values of S_D and S_Q accordingly decrease. This illustrates the value of using the longest boom technically and economically possible.

SUMMARY AND CONCLUSION

An extension of the dual magnetometer method of Ness et al. (1971), applicable for data from a dual spinning spacecraft, has been described. The scheme exploits the facts that: (1) the stationary segment of the spacecraft contains a magnetic field source (imaging system) which is strong and significantly offset from the spacecraft center and (2) the spinning segment is the platform for the magnetometer boom. Hence, dual magnetometer data used in conjunction with a dipole-quadrupole net spacecraft field model enables an accurate estimate of this field once every spin period; this field is expected to be quasi-stationary over a spin period. The estimated spacecraft field is then subtracted from the total measured field (spacecraft plus ambient) providing accurate estimates of the ambient field for each detail sample. The method used in association with standard instrument zero level correction techniques should reduce the net error on the ambient field estimate to $\approx \pm 0.09\gamma$ per axis when a modest length boom (7-10m) is employed. Likewise the method provides the ability to achieve moderately good accuracy even for the case of the short boom (6 m) under those conditions when the longer boom is technically or economically prohibitive.

APPENDIX

An estimate of the error caused by neglecting the term containing the g_2^0 coefficient in equation 8 is made here. For completeness, equations 8, 9, and 10 are examined to ascertain the relative contributions of all terms, but initially only the field due to the imaging system is considered.

The spherical harmonic coefficients (g_i^j, h_i^j) for an expansion made about a center, C, are related to the components (M_x, M_y, M_z) of an offset tilted dipole (which represents the imaging system) by the following transformation (Bartels, 1936), given here to second order:

$$g^0_1 = M_z, \quad g^1_1 = M_x, \quad h^1_1 = M_y,$$

$$g^0_2 = (2\, M_z\, \Delta z - M_x\, \Delta x - M_y\, \Delta y)/a,$$

$$g^1_2 = (M_x\, \Delta z + M_z\, \Delta x)\, \sqrt{3}/a,$$

$$g^2_2 = (M_x\, \Delta x - M_y\, \Delta y)\, \sqrt{3}/a,$$

$$h^1_2 = (M_y\, \Delta z + M_z\, \Delta x)\, \sqrt{3}/a,$$

and

$$h^2_2 = (M_y\, \Delta x + M_x\, \Delta y)\, \sqrt{3}/a,$$

where $\vec{R} = (\Delta x, \Delta y, \Delta z)$ is the displacement vector between the point C and the center of the imaging system's moment, and a is a length scale normalization factor. These transformation equations are now used with the specific characteristics given in Table 1 for the JOP imaging system to estimate the relative order of magnitudes of the terms in equations 8, 9, and 10. In the following expressions, the brackets represent the

relative order-of-magnitudes (i.e. harmonic amplitudes) and the subscripts denote the dipole terms (D) or quadrupole terms (Q), excluding the g_2^0 term which is presented separately. First the r_2 = 7 m outer magnetometer standoff position is considered. The spacecraft field components are then estimated:

$$[(\frac{r_2}{a})^3 B_x^t] = [1930]_{D_x} + [700]_{Q_x} + [108]_{g_2^0}$$

$$[(\frac{r_2}{a})^3 B_y^t] = [966]_{D_y} + [467]_{Q_y}$$

$$[(\frac{r_2}{a})^3 B_z^t] = [259]_{D_z} + [605]_{Q_z} .$$

The g_2^0 term is the smallest and is $\approx$ 1/18 the D_x term and $\approx$ 1/7 the Q_x term. When r_2 = 10 m we obtain:

$$[490]_{Q_x}, [327]_{Q_y}, [424]_{Q_z}, \text{ and } [76]_{g_2^0},$$

where the dipole terms remain the same as for the r_2 = 7 m case. Again the g_2^0 term is the smallest and is $\approx$1/25 the D_x term and $\approx$ 1/7 the Q_x term.

In a similar manner, the absolute values of the constant g_2^0 term for the two cases can be obtained, and are 0.048γ and 0.011γ for r_2 = 7 and 10 m, respectively. Thus, for the imaging system alone, and for the characteristics given in Table 1, the g_2^0 term is clearly negligible.

For the centered spinning dipole of Table 1, $\vec{R} = 0$, which yields a g_2^0 term of zero. Also for the stationary "axial" dipole of Table 1 the resulting g_2^0 term is considerably smaller than the g_2^0 term of the imaging system, because $M_S \ll M_{IS}$, (D=) $\Delta z_S \approx \Delta z_{IS}/2$ and $\Delta x_S = \Delta y_S = 0$. Hence, neglecting the g_2^0 term for the net field of the JOP spacecraft is justified.

ACKNOWLEDGEMENT

We wish to thank Dr. M. Acuna for helpful comments and R. Thompson and L. Moriarty for computer programming assistance.

REFERENCES

Bartels, J., The Eccentric Dipole Approximating the Earth's Magnetic Field, Terrestrial Magnetism and Atmospheric Elec., 41, 225, 1936.

Lepping, R.P., Behannon, K.W., and Howell, D.R., A Method of Estimating Zero Level Offsets for a Dual Magnetometer with Flipper on a Slowly Rolling Spacecraft: Application to Mariner 10, NASA/GSFC X-692-75-268, October 1975.

Ness, N.F., Magnetometers for Space Research, Space Sci. Rev., 11, 111, 1970.

Ness, N.F., Behannon, K.W., Lepping, R.P., and Schatten, K.H., Use of Two Magnetometers for Magnetic Field Measurements on a Spacecraft, J. Geophys. Res., 76, 3564, 1971.

Ness, N.F., Behannon, K.W., Lepping, R.P., Whang, Y.C., and Schatten, K.H., Magnetic Field Observations near Venus: Preliminary Results from Mariner 10, Science, 183, 1301, 1974.

Schmidt, A., Der Magnetische Mittelpunkt der Erde und Seine Bedentung, Gerlands, Beiti. Geophys. 41, 346, 1937.

FIGURE CAPTION

Figure 1. Simulated spacecraft magnetic field error estimates as a function of the (equatorial) azimuthal angle ϕ. The imaging system is located at $\phi = 0^{o}$. The designations 7 and 10 refer to the net standoff distance of the outer magnetometer for the two tests, and S_T, S_D and S_Q are defined in the text. $\Gamma \equiv$ gauss.

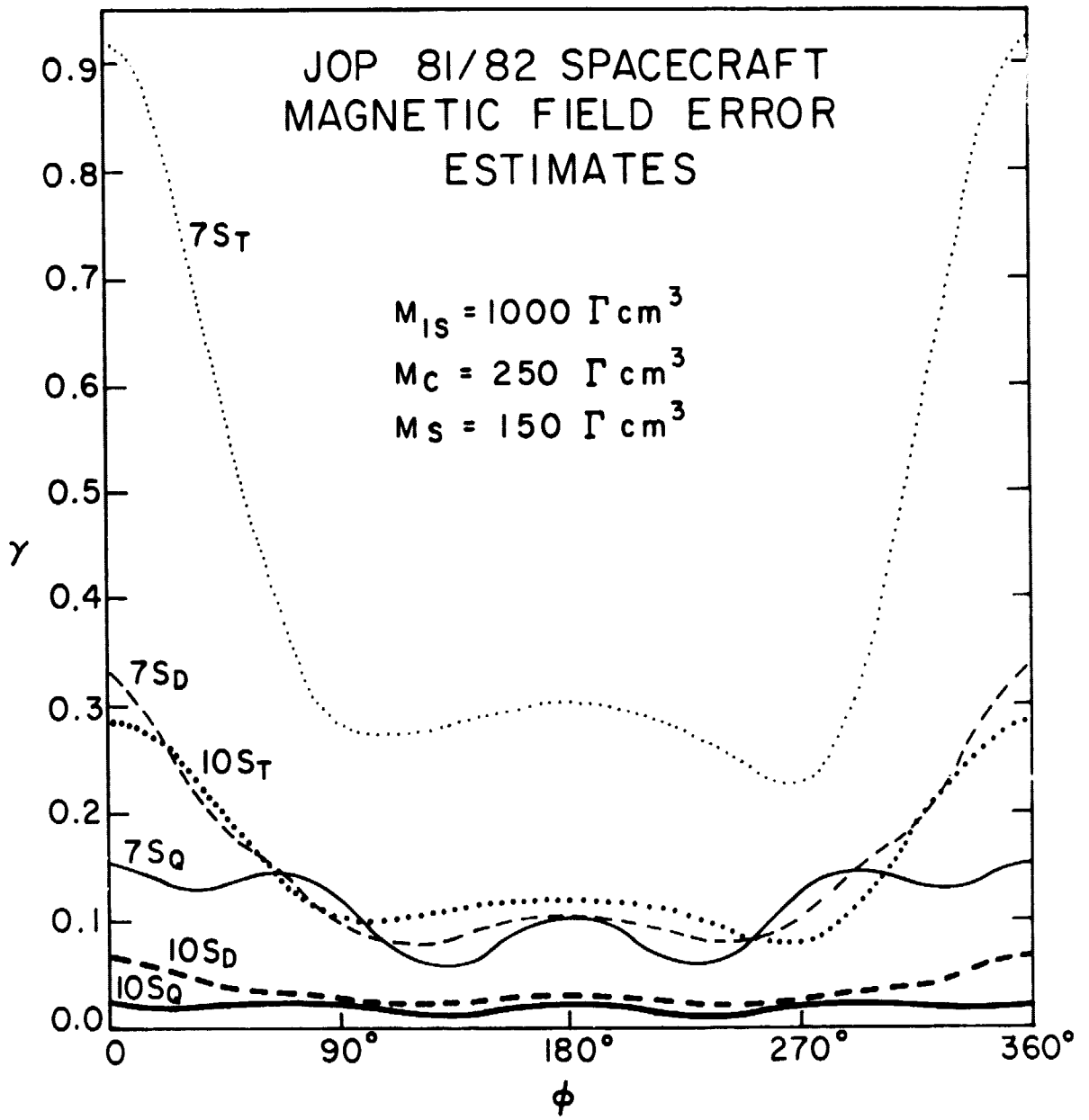
JOP 81/82 SPACECRAFT
MAGNETIC FIELD ERROR
ESTIMATES
M_{IS} = 1000 Γ cm^3
M_C = 250 Γ cm^3
M_S = 150 Γ cm^3
7S$_T$
7S$_D$
10S$_T$
7S$_Q$
10S$_D$
10S$_Q$
γ
0.0
0.1
0.2
0.3
0.4
0.5
0.6
0.7
0.8
0.9
0
90°
180°
270°
360°
φ

FIGURE 1